20th Australian International Aerospace Congress

ISBN number: 978-1-925627-66-4

Please select category below:
Normal Paper ☒
Student Paper ☐
Young Engineer Paper ☐

DSTG Planet Gear Rim Crack Propagation Test

David M. Blunt [1], Wenyi Wang [1], Lucinda Le Bas [2], Riyazal Hussein [1], Peter Stanhope [1]
George Jung [1], Elizabeth Hinchey [3], Eric Lee [1], Greg Surtees [1], Nicholas Athiniotis [1] and Scott Moss [1]

[1] *Platforms Division, Defence Science and Technology Group, 506 Lorimer Street, Port Melbourne, Victoria, 3207, Australia*
[2] *Contractor, Defence Science and Technology Group, 506 Lorimer Street, Port Melbourne, Victoria, 3207, Australia,*
[3] *Defence Graduate Program, Department of Defence, Australia*

Abstract

The Defence Science and Technology Group (DSTG) recently conducted a planet gear fatigue crack propagation test in a Kiowa 206B-1 helicopter main rotor gearbox (4-planet version). This test was designed to explore the phenomenon of fatigue cracking in thin-rim helicopter planet gears where the gear body incorporates the outer raceway of the planet bearing, and the crack initiates at or near the raceway surface and propagates through the gear body instead of a gear tooth. The crack was initiated from an electric discharge machined (EDM) notch in the planet gear rim and propagated from one side of the gear to the other between two gear teeth. This type of fault is challenging to detect reliably due to the lack of liberated wear debris, and the relatively weak vibration signature (using classical vibration fault detection methods) until the crack reaches across a large proportion of the gear body. As a result, this can lead to the catastrophic failure of the main rotor gearbox. The details of the test, selected results, and other issues are presented and discussed. A vibration dataset generated from this test was made available to the participants of HUMS2023 conference for a data challenge competition.

Keywords: fatigue crack, fault detection, helicopter, planetary gearbox, planet gear.

Introduction

Helicopters usually have one or more epicyclic stages in the main rotor gearbox. This allows the high torque load of the main rotor to be shared between multiple planet gears. Typically, the sun gear is the input, the planet carrier is the output, and the ring (annulus) gear is stationary.

Detecting faults in epicyclic gears is difficult; particularly for those that do not shed metal, such as fatigue cracks. This can lead to catastrophic failures, even in helicopters with relatively sophisticated health and usage monitoring systems (HUMS). In two recent examples [1, 2], a fatigue crack initiated at the inner bore surface of a planet gear (outer bearing raceway) and propagated through the body of the gear until it fractured into pieces, with the resulting secondary damage causing the separation of the main rotor from the helicopter.

The method most often used to detect fatigue cracks in gears is vibration analysis. Many detection algorithms have been developed over the years and proven successful at detecting cracks in fixed-axis gears [3-6]. However, these algorithms are typically less effective when applied to epicyclic gear trains for three general reasons:

a) There are multiple planet gears. Each planet meshes with both the sun and ring gears, and each mesh generates vibration at the same frequencies. The vibration from the healthy meshes mask the fault signature from the defective gear.
b) The phasing of the vibration from each gear mesh may result, when summed across all epicyclic sources, in near-cancellation of some frequency components, and unusual spectral structures [7].
c) The planet gears 'orbit' around the sun gear. This creates multiple time-varying transmission paths to external vibration sensors, and significant signal modulations.

To make matters worse, a crack in the gear body may initially cause a smaller disturbance to the meshing vibration than, for example, a cracked tooth. This could result in the crack not being detected until it reaches across a significant proportion of the gear body, at which point the whole gear will be in danger of suddenly breaking apart.

The primary objective of this test was therefore to record a large vibration dataset from many different sensors while propagating a fatigue crack through the body of a planet gear in a controlled and safe manner. A retired Kiowa 206B-1 main rotor gearbox (4-planet version) was used as the test article for this test, as it is representative of the general transmission layout of many helicopter main rotor gearboxes.

Planet Gear Defects and Load Cycle

To initiate the fatigue crack, two stress-raising EDM notches were inserted in the gear, as shown in Figs. 1 and 2. Two notches were used because the first (smaller) notch did not initiate a crack during the first 146 load cycles of the test. This was confirmed by disassembly of the gearbox and eddy-current non-destructive testing of the planet gear at that time. A second (larger) notch was then added in the same plane as the first on the opposite side of the gear. A fatigue crack was successfully initiated and propagated from the second notch over load cycles 147 – 241. The notches were approximately 0.14 mm to 0.20 mm wide, with the second notch visually wider than the first. The fillet radius at the bottom of the notch was assumed to be 0.02 mm. The notch shapes and sizes were guided by two sets of finite element analysis (FEA) [8, 9]: one conducted pre-test, and one after the disassembly at 146 cycles. The first FEA predicted a peak local stress at the notch just below the yield strength of the gear material. The second FEA predicted a peak stress in the second notch above the yield strength.

The test was undertaken using the loading cycle shown in Table 1. The table excludes the time required to adjust the torque in between each setting (roughly 40 – 60 seconds). Most of time in each load cycle was spent in an overload condition to accelerate the crack propagation. After cycle 9, a better data acquisition rhythm was established, and the durations at the lower loads were shortened and the time at 125% increased. Based on prior experience with this gearbox, loads were not increased beyond 125% in order to minimise the possibility of the planet roller bearings spalling. The load cycle was not meant to represent a flight profile. The lower torque values were incorporated to collect data at those torques and to add progression (beach) marks into the fracture surface. The load percentage is an estimate of the nominal rated load.

Instrumentation

The gearbox was instrumented with four single-axis Endevco 6259M6-10 accelerometers and one tri-axial Endevco 2258A-100 accelerometer (Fig. 3). Inductive pick-ups provided 1/rev and 128/rev tachometer signals on the input and output shafts. Analogue voltage signals

proportional to the input torque, oil pressure, oil temperature and mast vertical loads were also generated. The analogue test instrumentation signals (Table 2) were passed through a BNC patch panel to two separate recording systems: a Brüel and Kjær LAN-XI system connected to one computer; and a National Instruments PXI system connected to a second computer that was running a Matlab-based analysis GUI set up to monitor the test in near real-time. The Data Challenge data were derived from the PXI system, as it collected data more frequently than the LAN-XI system, but only at the 125% load condition. The LAN-XI system collected 90-second recordings from all signals at all loads, but it only collected data at the start and near the end of the 125% load condition, not at any intermediary points of this stage. Lastly, a Gastops MetalSCAN (Model 2201) inductive wear debris monitor plumbed into the oil scavenge line between the oil pump and oil filter was connected to a third computer.

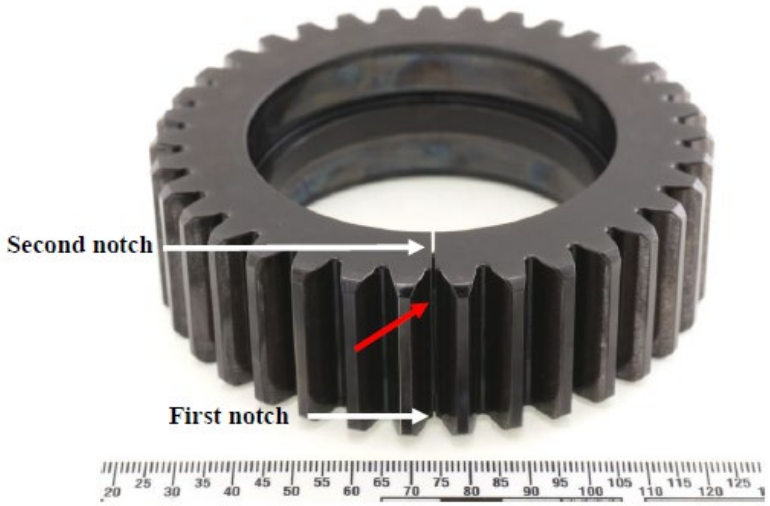

Fig. 1: The planet gear (crack indicated by red arrow)

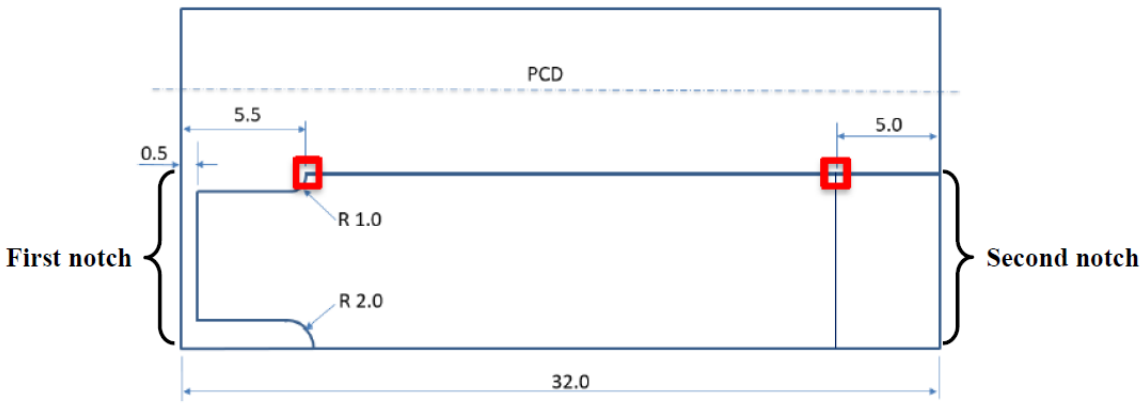

Fig. 2: Planet gear notches (dim. in mm); dashed line indicates the approx. position of the pitch circle diameter (PCD); FEA stress extracted from red highlights [10]

Table 1: Loading cycle

#	Load	Input Torque (Nm)	Input speed	Duration (cycles 1-9)	Duration (cycles 10-241)
A	50%	152	6000 RPM	3 minutes	2 minutes
B	75%	227	6000 RPM	3 minutes	2 minutes
C	100%	303	6000 RPM	3 minutes	2 minutes
D	125%	379	6000 RPM	21 minutes	24 minutes

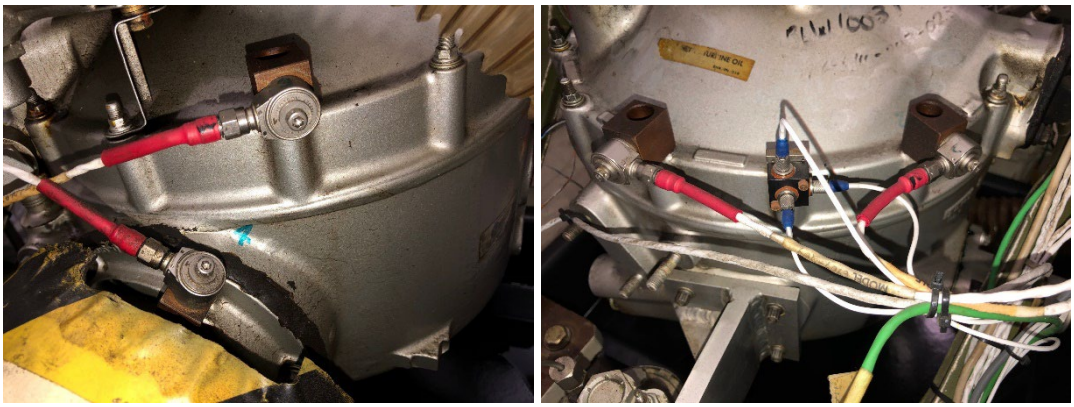

Fig. 3: Accelerometers as mounted on the gearbox

Table 2: LAN-XI channels (indicates channel also recorded on PXI system)*

Chan	Description	Chan	Description
1	Input speed – 128/rev	10	Tri-axial accel. – X
2*	Input speed – 1/rev	11	Tri-axial accel. – Y
3	Rotor speed – 128/rev	12	Tri-axial accel. – Z
4	Rotor speed – 1/rev	13	Lube oil pressure out
5*	Input pinion / bevel gear	14	Lube oil temperature out
6*	Ring gear accel. – front	15*	Input torque
7*	Ring gear accel. – side	16	Vertical mast load 1
8*	Ring gear accel. – rear	17	Vertical mast load 2
9	Drive motor step-up gearbox	18	Not connected

LAN-XI sample rate = 65536 Hz (bandwidth = 25600 Hz), *PXI sample rate = 65573.77 Hz

Experimental Test Summary

The test was undertaken in the Helicopter Transmission Test Facility at DSTG Melbourne. Due to the COVID-19 pandemic, the test was conducted on 27 separate days spread over a prolonged period (Table 3). There was an extended break in testing from Jan to Oct 2021 where: the gearbox was disassembled; additional FEA was undertaken; the second notch was machined; and the gearbox reassembled.

The ferromagnetic debris counts detected by the inductive wear debris monitor for the second part of the test are shown in Fig. 4. Ignoring the major breaks in testing (shaded), it can be seen that the largest count increases were detected on the first two runs after gearbox reassembly (25 Oct & 15 Nov); however, this was considered normal behaviour following reassembly. There was then a long relatively stable period leading up to the last two test days, with only a few counts accumulating in the smallest bin size. The final 10 particles (in the 250 µm and 400 µm bins) may have been liberated as the crack broke through to the first notch which, by that time, was slightly misaligned with the position of the crack front. It can be seen in Fig. 6 that some gear material was liberated from the bearing raceway side of the gear. No non-ferromagnetic particles were counted during this period.

One of the two magnetic chip detectors in the gearbox sump illuminated on the last day. Ten of the larger chip detector particles were analysed in a scanning electron microscope (SEM). Most were not gear or bearing steel. The long thin strand that triggered the detector was one of two gear steel particles, but the morphologies these particles were not consistent with the planet gear defect. Hence, there was no clear evidence of the fatigue crack from the particles. Note that sump chip-detector particles did not pass through the inductive wear debris monitor.

Table 3: Experimental test dates

Notch	Cycle #	Days	Month	Year
1	1-8, 9-17, 18-24, 25-32, 33-41, 42-49, 50-57	3,9,12,16,17,25,26	Jun	2020
	58-64, 65-72	16, 17	Jul	
	73-82, 83-93, 94-104, 105-114	18, 23, 25, 30	Nov	
	115-125, 126-136, 137-146	2, 7, 9	Dec	
1 & 2	30 min. low-load run after re-assembly	25	Oct	2021
	147-154, 155-163, 164-171	15, 18, 24	Nov	
	172-181, 182-191, 192-200, 201-208, 209-218	2, 8, 9, 14, 16	Dec	
	219-228, 229-238, 239-241	11, 14, 18	Jan	2022

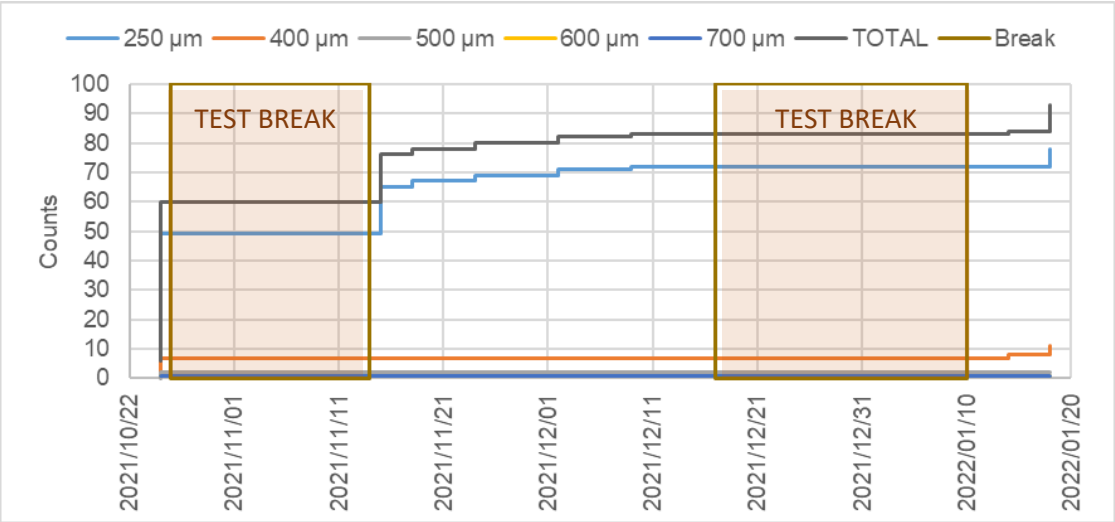

Fig. 4: Ferromagnetic debris counts (no particles in bins above 700µm)

The (near) real-time vibration monitoring was based on a number of relatively standard condition indices (CIs) calculated from the raw vibration data and the synchronous signal averages. Fig. 5 is a reconstruction of the GUI display on the final day of testing that illustrates the point where the crack broke through to the first notch. While this obviously produced a very large indication at the point of breakthrough, the trends of all the monitored CIs leading up to this point were much weaker. The test was then terminated in a controlled manner as quickly as possible. Firstly, the torque was reduced to zero, then the speed was reduced to zero.

Fracture Surface Analysis

The cracked planet gear is shown in Fig. 6 just after the completion of the test and removal from the gearbox. It was clearly evident that the crack had propagated across the entire gear. When sectioned, the gear revealed a complex fracture surface (Fig. 7) with multiple fatigue origins along the edge of the second notch [10]. Enlarged views of the two opposing fracture surface faces are shown in Fig. 8. Examination of the fracture surface was challenging because the fatigue progression marks were not clear, as is typical for steel fatigue fractures. No identifiable fatigue markings could be seen originating from the first notch. Only 65 cycles could be identified in the crack initiated from the second notch: cycles 148-158 (from SEM images); and cycles 186-201 and 204-241 (from optical microscope images). The fracture surface analysis yielded the crack propagation shown in Fig. 10. It can be seen that the growth rate was relatively slow until around cycle 180. There was a relatively linear growth rate through cycles 186 to 232, and then a rapid acceleration from there to the final cycle.

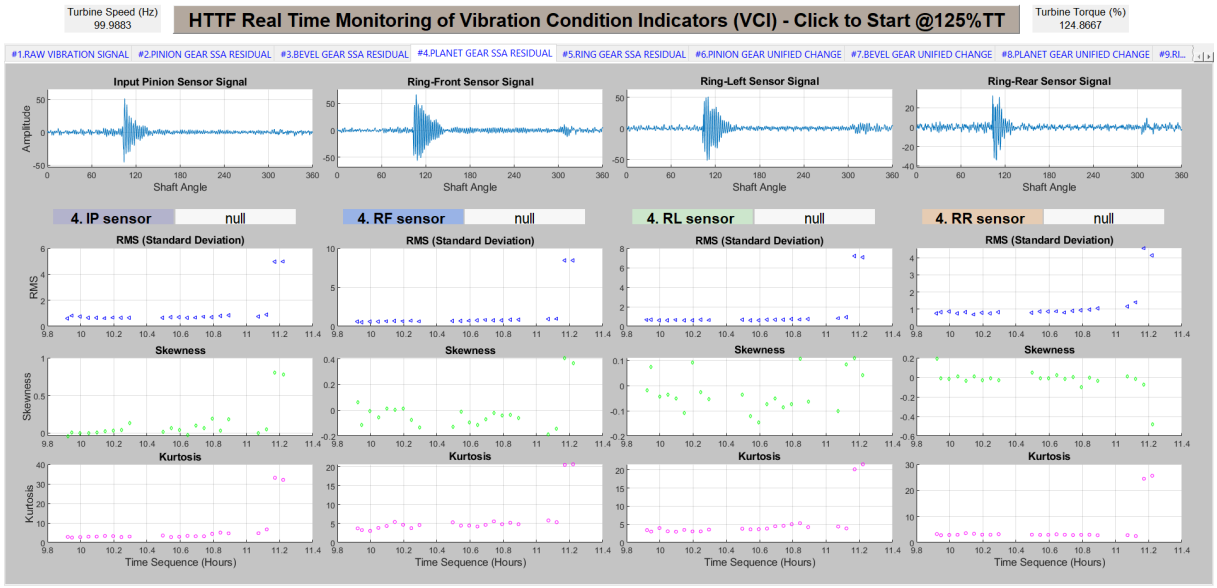

Fig. 5: Real-time GUI indicators for the final test day showing step change towards the end rows 1–4: = planet gear residual signals, residual RMS, residual skewness, residual kurtosis cols 1–4: input pinion, ring-front, ring left-side and ring-rear accelerometers

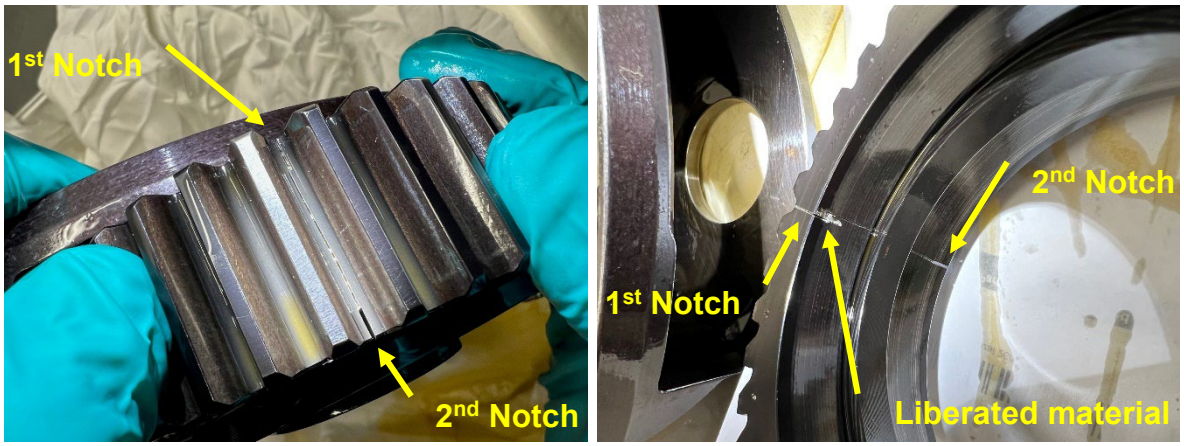

Fig. 6: Cracked planet gear outer (left) and inner (right) views

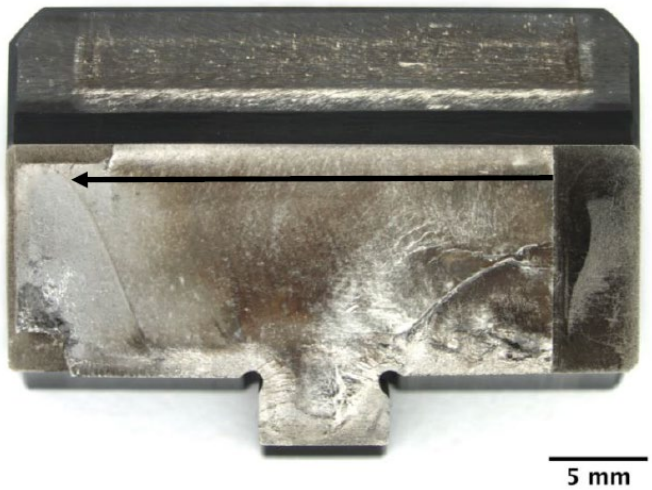

Fig. 7: Overall view of the fracture surface – the arrow indicates the approx. crack length measurement location and points to the final curved beach mark (the low load of cycle 241)

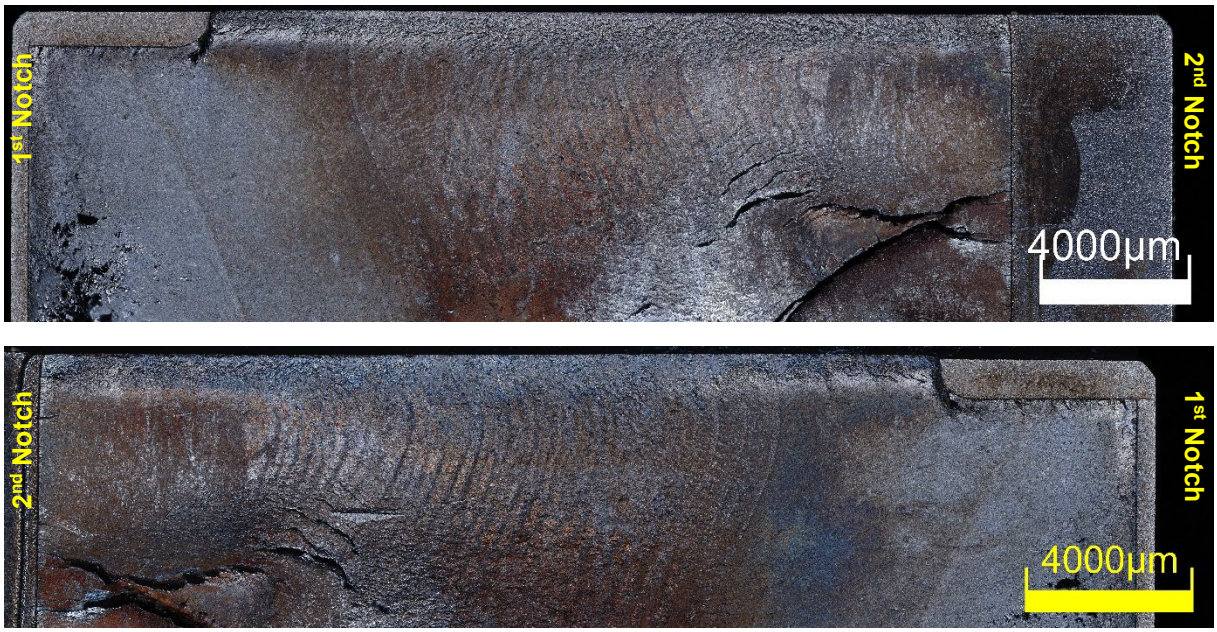

Fig. 8: Enlarged views of the two opposing fracture surface faces

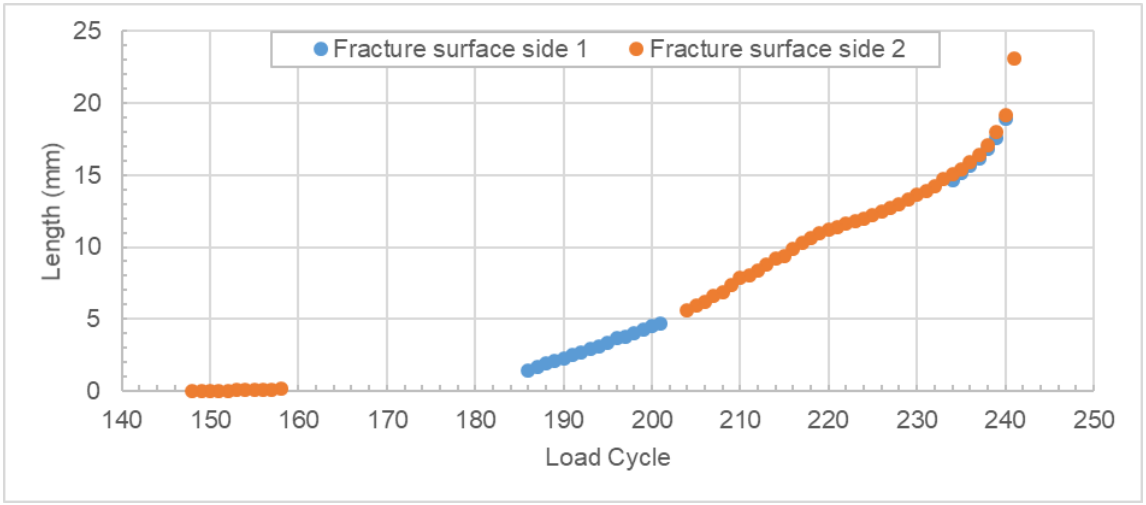

Fig. 9: Fatigue crack propagation from SEM and optical imaging

Concluding Remarks

A fatigue crack propagation test was successfully conducted in a planet gear of a 4-planet Kiowa main rotor gearbox. Stress raising notches were used to initiate the crack. A larger second notch was required after the first failed to initiate a crack after 146 load cycles. The crack initiated from the second notch and propagated to the first notch over 95 load cycles. There were three phases of crack growth: initial slow growth; a period of relatively linear growth; and an accelerating rapid rate of growth over the last 9 load cycles.

There were no obvious indications of the crack growth during the test from the real-time vibration or wear debris monitoring until the last test day. This can be attributed to a combination of the difficulty in detecting faults in epicyclic gears in general, and to the fundamental nature of this specific type of fault in particular. However, further more advanced vibration analysis will be undertaken in the future to see if these results can be improved upon. A repeat test may also be conducted with additional instrumentation.

Acknowledgments

Guido Papp and Damion Hadcroft (QinetiQ, Australia) for the FEA analyses of the planet gear. Dr Andrew Becker (DSTG) for wear debris analysis.

References

1. *Aircraft Accident Report 2/2011 - Aerospatiale (Eurocopter) AS332 L2 Super Puma, G-REDL, 1 April 2009*, Air Accidents Investigation Branch, Department for Transport, UK, 2014. Accessed 15 September 2022. Available from: https://www.gov.uk/aaib-reports/2-2011-aerospatiale-eurocopter-as332-l2-super-puma-g-redl-1-april-2009.
2. *Report on the air accident near Turøy, Øygarden municipality, Hordaland county, Norway 29 April 2016 with Airbus Helicopters EC 225 LP, LN-OJF, operated by CHC Helikopter Service AS*, Norwegian Safety Investigation Authority, 2018. Accessed 15 September 2022. Available from: https://www.nsia.no/Aviation/Published-reports/2018-04.
3. Forrester, B.D., *Advanced Vibration Analysis Techniques for Fault Detection and Diagnosis in Geared Transmission Systems*, Ph.D. Thesis, Swinburne University of Technology, Melbourne, Australia, 1996.
4. Forrester, B.D. and D.M. Blunt, *Analysis of Epicyclic Gearbox Vibration*, in *DSTO International Conference on Health and Usage Monitoring*, 2003, Melbourne, Australia.
5. Wang, W., B.D. Forrester, and P.C. Frith, *A unified approach to detecting and trending changes caused by mechanical faults in rotating machinery.* Structural Health Monitoring, 2016, **15**(2), p. 204-222 DOI: 10.1177/1475921716636337.
6. Becker, A., D.M. Blunt, and B.D. Forrester, *A review of permanently installed helicopter gearbox vibration monitoring systems in the Australian Defence Force*, in *DSTO International Conference on Health and Usage Monitoring*, 2001, Melbourne, Australia.
7. Molina Vicuña, C., *Theoretical frequency analysis of vibrations from planetary gearboxes.* Forsch Ingenieurwes, 2012, **76**, p. 15-31 DOI: 10.1007/s10010-012-0151-1.
8. Papp, G., *Finite Element Analysis of Planet Gear*, Report No. ER-DSTO-501-QES054, QinetiQ, 2017, QinetiQ Pty. Ltd., South Melbourne, Australia.
9. Hadcroft, D., *Notched planet gear FEA*, Report No. QPL-LR-01066, QinetiQ, 2021, Q.P. Ltd., South Melbourne, Australia.
10. Le Bas, L., *HTTF Planet Gear Fatigue Crack Investigation*, Report No. DSTG/AFE/20226594, DSTG, 2022.